CLNS 09/2052
CLEO 09-05

Inclusive Hadron Yields from D_s^+ Decays

S. Dobbs,[1] Z. Metreveli,[1] K. K. Seth,[1] B. J. Y. Tan,[1] A. Tomaradze,[1] J. Libby,[2] L. Martin,[2] A. Powell,[2] C. Thomas,[2] G. Wilkinson,[2] H. Mendez,[3] J. Y. Ge,[4] D. H. Miller,[4] I. P. J. Shipsey,[4] B. Xin,[4] G. S. Adams,[5] D. Hu,[5] B. Moziak,[5] J. Napolitano,[5] K. M. Ecklund,[6] Q. He,[7] J. Insler,[7] H. Muramatsu,[7] C. S. Park,[7] E. H. Thorndike,[7] F. Yang,[7] M. Artuso,[8] S. Blusk,[8] S. Khalil,[8] R. Mountain,[8] K. Randrianarivony,[8] T. Skwarnicki,[8] S. Stone,[8] J. C. Wang,[8] L. M. Zhang,[8] G. Bonvicini,[9] D. Cinabro,[9] M. Dubrovin,[9] A. Lincoln,[9] M. J. Smith,[9] P. Zhou,[9] J. Zhu,[9] P. Naik,[10] J. Rademacker,[10] D. M. Asner,[11] K. W. Edwards,[11] J. Reed,[11] A. N. Robichaud,[11] G. Tatishvili,[11] E. J. White,[11] R. A. Briere,[12] H. Vogel,[12] P. U. E. Onyisi,[13] J. L. Rosner,[13] J. P. Alexander,[14] D. G. Cassel,[14] R. Ehrlich,[14] L. Fields,[14] L. Gibbons,[14] R. Gray,[14] S. W. Gray,[14] D. L. Hartill,[14] B. K. Heltsley,[14] D. Hertz,[14] J. M. Hunt,[14] J. Kandaswamy,[14] D. L. Kreinick,[14] V. E. Kuznetsov,[14] J. Ledoux,[14] H. Mahlke-Krüger,[14] J. R. Patterson,[14] D. Peterson,[14] D. Riley,[14] A. Ryd,[14] A. J. Sadoff,[14] X. Shi,[14] S. Stroiney,[14] W. M. Sun,[14] T. Wilksen,[14] J. Yelton,[15] P. Rubin,[16] N. Lowrey,[17] S. Mehrabyan,[17] M. Selen,[17] J. Wiss,[17] M. Kornicer,[18] R. E. Mitchell,[18] M. R. Shepherd,[18] C. Tarbert,[18] D. Besson,[19] T. K. Pedlar,[20] J. Xavier,[20] D. Cronin-Hennessy,[21] K. Y. Gao,[21] J. Hietala,[21] T. Klein,[21] R. Poling,[21] and P. Zweber[21]

(CLEO Collaboration)

[1]*Northwestern University, Evanston, Illinois 60208, USA*
[2]*University of Oxford, Oxford OX1 3RH, United Kingdom*
[3]*University of Puerto Rico, Mayaguez, Puerto Rico 00681*
[4]*Purdue University, West Lafayette, Indiana 47907, USA*
[5]*Rensselaer Polytechnic Institute, Troy, New York 12180, USA*
[6]*Rice University, Houston, Texas 77005, USA*
[7]*University of Rochester, Rochester, New York 14627, USA*
[8]*Syracuse University, Syracuse, New York 13244, USA*
[9]*Wayne State University, Detroit, Michigan 48202, USA*
[10]*University of Bristol, Bristol BS8 1TL, United Kingdom*
[11]*Carleton University, Ottawa, Ontario, Canada K1S 5B6*
[12]*Carnegie Mellon University, Pittsburgh, Pennsylvania 15213, USA*
[13]*Enrico Fermi Institute, University of Chicago, Chicago, Illinois 60637, USA*
[14]*Cornell University, Ithaca, New York 14853, USA*
[15]*University of Florida, Gainesville, Florida 32611, USA*
[16]*George Mason University, Fairfax, Virginia 22030, USA*
[17]*University of Illinois, Urbana-Champaign, Illinois 61801, USA*
[18]*Indiana University, Bloomington, Indiana 47405, USA*
[19]*University of Kansas, Lawrence, Kansas 66045, USA*
[20]*Luther College, Decorah, Iowa 52101, USA*
[21]*University of Minnesota, Minneapolis, Minnesota 55455, USA*

(Dated: April 15, 2009)

Abstract

We study the inclusive decays of D_s^+ mesons, using data collected near the $D_s^{*+}D_s^-$ peak production energy $E_{\rm cm} = 4170$ MeV by the CLEO-c detector. We report the inclusive yields of D_s^+ decays to K^+X, K^-X, K_S^0X, π^+X, π^-X, π^0X, ηX, $\eta' X$, ϕX, ωX and $f_0(980)X$, and also decays into pairs of kaons, $D_s^+ \to K\bar{K}X$. Using these measurements, we obtain an overview of D_s^+ decays.

The D_s^+ meson, consisting of a c and $\bar{s}$ quark, is the least extensively studied of the ground state charmed mesons. Here we present measurements of many inclusive yields from D_s^+ decay, thereby obtaining an overview of D_s^+ decays.

Studies of inclusive branching fractions provide strong constraints on Monte Carlo simulation. On completion of the measurements described here, we retuned our Monte Carlo decay table. The comparisons of Monte Carlo and data yields and spectra given below are *after* this retuning.

In addition to providing an improved Monte Carlo decay table, our results allow some comparisons with expectations.

Data for this analysis were taken at the Cornell Electron Storage Ring (CESR) using the CLEO-c general-purpose solenoidal detector, which is described in detail elsewhere [1–4]. The charged particle tracking system covers a solid angle of 93% of 4π and consists of a small-radius, six-layer, low-mass, stereo wire drift chamber, concentric with, and surrounded by, a 47-layer cylindrical central drift chamber. The chambers operate in a 1.0 T magnetic field and achieve a momentum resolution of $\sim$0.6% at p =1 GeV/c. Photons are detected in an electromagnetic calorimeter consisting of 7800 cesium iodide crystals and covering 95% of 4π, which achieves a photon energy resolution of 2.2% at E_γ =1 GeV and 6% at 100 MeV. We utilize two particle identification (PID) devices to separate charged kaons from pions: the central drift chamber, which provides measurements of ionization energy loss (dE/dx), and, surrounding this drift chamber, a cylindrical ring-imaging Cherenkov (RICH) detector, whose active solid angle is 80% of 4π. The combined PID system has a pion or kaon efficiency $>$ 85% and a probability of pions faking kaons (or vice versa) $<$ 5% [5]. The detector response is modeled with a detailed GEANT-based [6] Monte Carlo (MC) simulation, with initial particle trajectories generated by EvtGen [7] and final state radiation produced by PHOTOS [8]. The initial-state radiation is modeled using cross sections for $D_s^{*\pm}D_s^{\mp}$ production at lower energies obtained from the CLEO-c energy scan [9] near the CM energy where we collect the sample.

We use 586 pb^{-1} of data produced in e^+e^- collisions at CESR near the center-of-mass energy $\sqrt{s} = 4170$ MeV. Here the cross-section for the channel of interest, $D_s^{*+}D_s^-$ or $D_s^+D_s^{*-}$, is $\sim$1 nb [9]. We select events in which the D_s^* decays to $D_s\gamma$ (94% branching fraction [10]). Other charm production totals $\sim$7 nb [9], and the underlying light-quark "continuum" is about 12 nb.

Here we employ a double-tagging technique. Single-tag (ST) events are selected by fully reconstructing a D_s^-, which we call a tag, in one of the following three two-body hadronic decay modes: $D_s^- \to K_S^0K^-$, $D_s^- \to \phi\pi^-$ and $D_s^- \to K^{*0}K^-$. (Mention of a specific mode implies the use of the charge conjugate mode as well throughout this paper.) Details on the tagging selection procedure are given in Ref. [11]. The tagged D_s^- candidate can be either the primary D_s^- or the secondary D_s^- from the decay $D_s^{*-} \to \gamma D_s^-$. We require the following intermediate states to satisfy these mass windows around the nominal mass [10]: $K_S^0 \to \pi^+\pi^-$ ($\pm$12 MeV), $\phi \to K^+K^-$ ($\pm$10 MeV) and $K^{*0} \to K^+\pi^-$ ($\pm$75 MeV). All charged particles utilized in tags must have momenta above 100 MeV/c to eliminate the soft pions from $D^*\bar{D}^*$ decays (through $D^* \to \pi D$).

We use the reconstructed invariant mass of the D_s candidate, $M(D_s)$, and the mass recoiling against the D_s candidate, $M_{\rm recoil}(D_s) \equiv \sqrt{(E_0 - E_{D_s})^2 - (\mathbf{p}_0 - \mathbf{p}_{D_s})^2}$, as our primary kinematic variables to select a D_s candidate. Here $(E_0, \mathbf{p}_0)$ is the net four-momentum of the e^+e^- beams, taking the finite beam crossing angle into account, $\mathbf{p}_{D_s}$ is the momentum of the D_s candidate, $E_{D_s} = \sqrt{m_{D_s}^2 + \mathbf{p}_{D_s}^2}$, and m_{D_s} is the known D_s mass [10]. We require the re-

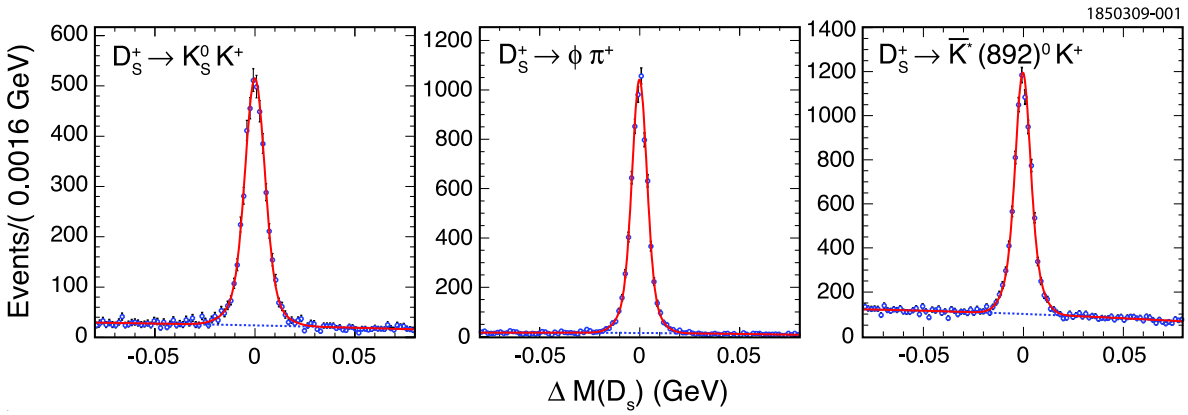

FIG. 1: The mass difference $\Delta M(D_s) \equiv M(D_s) - m_{D_s}$ distributions in each tag mode. We fit the $\Delta M(D_s)$ distribution (open circle) to the sum (solid curve) of signal (double-Gaussian) plus background (second degree polynomial, dashed curve) functions.

coil mass to be within 55 MeV of the D_s^* mass [10]. This loose window allows both primary and secondary D_s tags to be selected. We also require a photon consistent with coming from $D_s^* \to \gamma D_s$ decay, by looking at the mass recoiling against the D_s candidate plus γ system, $M_{\rm recoil}(D_s\gamma) \equiv \sqrt{(E_0 - E_{D_s} - E_\gamma)^2 - (\mathbf{p}_0 - \mathbf{p}_{D_s} - \mathbf{p}_\gamma)^2}$. For correct combinations, this recoil mass peaks at m_{D_s}, regardless of whether the candidate is due to a primary or a secondary D_s. We require $|M_{\rm recoil}(D_s\gamma) - m_{D_s}| < 30$ MeV.

The invariant mass distributions of D_s tag candidates for each tag mode are shown Fig. 1. We use the ST invariant mass sidebands to estimate the background in our signal yields from combinatorial background under the ST mass peaks. The signal region is $|\Delta M(D_s)| < 20$ MeV, while the sideband region is 35 MeV $< |\Delta M(D_s)| < 55$ MeV, where $\Delta M(D_s) \equiv M(D_s) - m_{D_s}$ is the difference between the tag mass and the nominal mass. To find the sideband scaling factor, the $\Delta M(D_s)$ distributions are fit to the sum of double-Gaussian signal plus second-degree polynomial background functions. We have 18586 $\pm$ 163 ST events that we use for further analysis.

In each event where a tag is identified, we search for our signal inclusive modes recoiling against the tag. Charged tracks utilized in signal candidates are required to satisfy criteria based on the track fit quality, have momenta above 50 MeV/c, and angles with respect to the beam line, θ, satisfying $|\cos\theta| < 0.80$. They must also be consistent with coming from the interaction point in three dimensions. Pion and kaon candidates are required to have dE/dx measurements within three standard deviations (3σ) of the expected value. For tracks with momenta greater than 700 MeV/c, RICH information, if available, is combined with dE/dx. Candidate positrons (and electrons), selected with criteria described in Ref. [12], are required to have momenta of at least 200 MeV/c.

For $D_s^+ \to K^+X$, $D_s^+ \to K^-X$, $D_s^+ \to \pi^+X$, and $D_s^+ \to \pi^-X$ modes, we count the numbers of charged kaons and pions recoiling against the tag where the tags are selected from both $M(D_s)$ signal and sideband regions. Thus the combinatoric background is subtracted by using $M(D_s)$ sideband events. The particle misidentification backgrounds among e, π and K are estimated by using the momentum-dependent particle misidentification rates determined from Monte Carlo and the e, π and K yields. Our identification can not distinguish between muons and pions. So, we assume the muon yield equals the electron yield, and subtract accordingly. For $D_s^+ \to \pi^+X$ and $D_s^+ \to \pi^-X$ modes, we treat $\pi^\pm$ from K_S^0

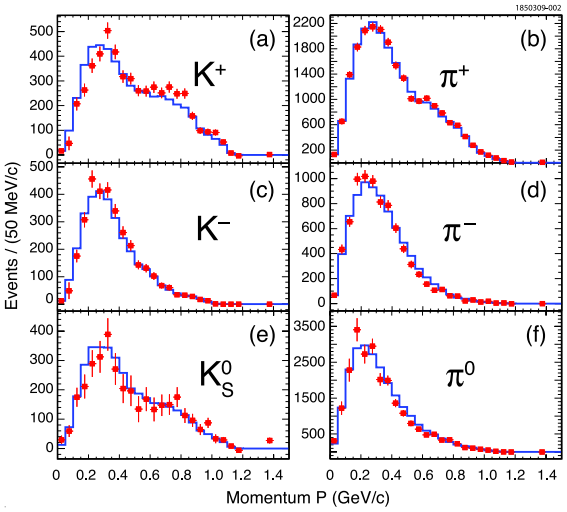

FIG. 2: Charged and neutral kaon and pion momentum spectra after background subtractions and efficiency corrections: (a) $D_s^+ \to K^+X$, (b) $D_s^+ \to \pi^+X$, (c) $D_s^+ \to K^-X$, (d) $D_s^+ \to \pi^-X$, (e) $D_s^+ \to K_S^0X$, (f) $D_s^+ \to \pi^0X$. The points are obtained from data and solid line indicates the Monte Carlo after tuning. Good agreement between data and tuned Monte Carlo is found. Monte Carlo is normalized to data based on tag yield.

decay as a background and subtract it based on K_S^0 yields. The momentum-dependent (50 MeV bins) efficiencies for track finding, track selection criteria, and particle identification are obtained from Monte Carlo simulation.

The K_S^0 candidates are reconstructed in $K_S^0 \to \pi^+\pi^-$ decay. The two pions have no PID requirements, and a vertex fit is done to allow for the K_S^0 flight distance. We identify π^0 candidates via $\pi^0 \to \gamma\gamma$, detecting the photons in the CsI calorimeter. We require that the calorimeter clusters have a measured energy above 30 MeV, have a lateral distribution consistent with that from photons, and not be matched to any charged track. The K_S^0 (or π^0) yield is extracted by defining a signal region and sideband regions in the invariant mass distribution of the pion (or photon) pair. The sideband scaling factor is obtained from Monte Carlo, thus allowing for a non-linear background shape. We treat π^0 from K_S^0 decay as a background for the decay $D_s^+ \to \pi^0X$ and subtract it based on K_S^0 yields.

The momentum spectra after all background subtractions and efficiency corrections are shown in Fig. 2

For the η we use the $\gamma\gamma$ final state, which has a large branching fraction in η decays. To better handle the mild dependence of efficiency on η momentum, we separate the η sample into two momentum ranges to measure the inclusive yields, one below 300 MeV/c and the other above. The η signal and background yields are determined by fits to a Crystal Ball function [13], to account for the peak and the low mass tail, and background polynomial. We reconstruct η' candidates in the the decay mode $\eta' \to \pi^+\pi^-\eta$ with the η subsequently decaying into $\gamma\gamma$. Candidates for η' are selected by combining η candidates within 3 r.m.s. widths of the nominal η mass, with a pair of $\pi^+\pi^-$. The mass difference between $\eta\pi^+\pi^-$ and η is then examined and fit to a Gaussian signal function and a background polynomial to extract the η' yields. The ϕ candidates are reconstructed in $\phi \to K^+K^-$ decay. We break the ϕ sample into several momentum regions (200 MeV/c bins) since the ϕ efficiency changes substantially with momentum. In each momentum region, the signals are fit with a

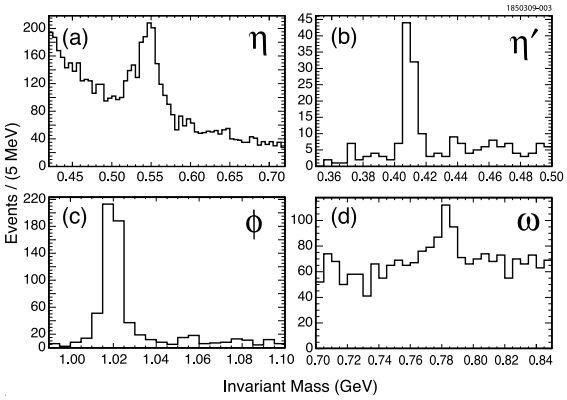

FIG. 3: Invariant mass distributions: (a) $D_s^+ \to \eta X$, (b) $D_s^+ \to \eta' X$, (c) $D_s^+ \to \phi X$, (d) $D_s^+ \to \omega X$.

sum of two Gausssian shapes and the background is fit to a polynomial. We reconstruct ω candidates in $\omega \to \pi^+\pi^-\pi^0$ decay and extract the ω signal yields from the $\pi^+\pi^-\pi^0$ invariant mass distribution. The invariant mass distributions of η, η', ϕ, and ω candidates, summed over all momenta, are shown in Fig. 3.

We form $f_0(980)$ candidates using $\pi^+\pi^-$ pairs, $f_0(980) \to \pi^+\pi^-$. The pions are subject to the standard pion PID requirements. We find no significant evidence for the decay $D_s^+ \to f_0(980)X$. We fit the invariant mass distribution of $\pi^+\pi^-$ pairs to a Gaussian signal function plus a second-degree polynomial background function and we obtain a yield of 30 ± 47. The 90% confidence level upper limit is $\mathcal{B}(D_s^+ \to f_0(980)X)\mathcal{B}(f_0(980) \to \pi^+\pi^-) < 1.1\%$ (statistical uncertainty only). Systematic errors are 6.8% for the efficiency estimation, 5.6% for the signal and background shape parameters, and other smaller errors, leading to a combined relative systematic error of 8.8%. We conservatively increase the upper limit by 1.28 times the combined systematic errors, giving a upper limit, including systematic errors, of $\mathcal{B}(D_s^+ \to f_0(980)X)\mathcal{B}(f_0(980) \to \pi^+\pi^-) < 1.3\%$.

We also measure the inclusive yields of D_s^+ mesons into two kaons. After a tag is identified, we search for the best kaon pair, based on particle identification likelihood or K_S^0 mass, per mode recoiling against the tag. The kaon pair modes can be any of $K_S^0K_S^0$, $K_S^0K^+$, $K_S^0K^-$, K^+K^-, K^+K^+ or K^-K^-. For $D_s^+ \to K_S^0K^+X$ and $D_s^+ \to K_S^0K^-X$, we apply the sideband subtraction on K_S^0 candidate invariant mass distribution to remove the non-resonant decay background and get the signal yields. The $D_s^+ \to K_S^0K_S^0X$ signal yield is extracted by defining a signal region on the scatter plot for the two K_S^0 candidate invariant masses. In order to account for $D_s^+ \to K_S^0\pi^+\pi^-X$ and $D_s^+ \to \pi^+\pi^-\pi^+\pi^-X$ entering into the signal region of $D_s^+ \to K_S^0K_S^0X$, we perform a background subtraction which has two components. For all two charged kaons modes, we count the event numbers where at lease two charged kaons are found recoiling against the tag. In order to subtract the combinatoric background, we repeat the same procedure for each mode where the tags are selected from $M(D_s)$ sidebands. The other possible backgrounds from generic D_s decay are studied using Monte Carlo and found to be negligible.

The double-tagging technique allows us to measure the inclusive yields for the decay $D_s^+ \to K_L^0X$ without directly detecting the K_L^0. Instead, we reconstruct all particles in the event except the single K_L^0 and infer the presence of a K_L^0 from the missing four-momentum. Our signal is a peak in the missing mass squared distribution at the K_L^0 mass squared. Similar missing-mass-squared techniques are used for $D_s^+ \to K_L^0K_S^0X$, $D_s^+ \to K_L^0K^+X$ and

TABLE I: D_s inclusive yield results. Uncertainties are statistical and systematic, respectively. The inclusive K_L^0 results are only used as a check for K_S^0. The $D_s^+ \to K_L^0 X$ yield requires a correction before comparing with the $D_s^+ \to K_S^0 X$ yield, as explained in the text. PDG [10] averages are shown in the last column, when available.

Mode	Yield(%)	K_L^0 Mode	Yield(%)	$\mathcal{B}$(PDG)(%)
$D_s^+ \to \pi^+ X$	$119.3 \pm 1.2 \pm 0.7$			
$D_s^+ \to \pi^- X$	$43.2 \pm 0.9 \pm 0.3$			
$D_s^+ \to \pi^0 X$	$123.4 \pm 3.8 \pm 5.3$			
$D_s^+ \to K^+ X$	$28.9 \pm 0.6 \pm 0.3$			$20\ ^{+\ 18}_{-\ 14}$
$D_s^+ \to K^- X$	$18.7 \pm 0.5 \pm 0.2$			$13\ ^{+\ 14}_{-\ 12}$
$D_s^+ \to \eta X$	$29.9 \pm 2.2 \pm 1.7$			
$D_s^+ \to \eta' X$	$11.7 \pm 1.7 \pm 0.7$			
$D_s^+ \to \phi X$	$15.7 \pm 0.8 \pm 0.6$			
$D_s^+ \to \omega X$	$6.1 \pm 1.4 \pm 0.3$			
$D_s^+ \to f_0(980)X, f_0(980) \to \pi^+\pi^-$	$< 1.3\%$ (90% CL)			
$D_s^+ \to K_S^0 X$	$19.0 \pm 1.0 \pm 0.4$	$D_s^+ \to K_L^0 X$	15.6 ± 2.0	20 ± 14
$D_s^+ \to K_S^0 K_S^0 X$	$1.7 \pm 0.3 \pm 0.1$	$D_s^+ \to K_L^0 K_S^0 X$	5.0 ± 1.0	
$D_s^+ \to K_S^0 K^+ X$	$5.8 \pm 0.5 \pm 0.1$	$D_s^+ \to K_L^0 K^+ X$	5.2 ± 0.7	
$D_s^+ \to K_S^0 K^- X$	$1.9 \pm 0.4 \pm 0.1$	$D_s^+ \to K_L^0 K^- X$	1.9 ± 0.3	
$D_s^+ \to K^+ K^- X$	$15.8 \pm 0.6 \pm 0.3$			
$D_s^+ \to K^+ K^+ X$	$< 0.26\%$ (90% CL)			
$D_s^+ \to K^- K^- X$	$< 0.06\%$ (90% CL)			

$D_s^+ \to K_L^0 K^- X$ modes by requiring there must be a K_S^0, K^+ or K^- recoiling against the tag. Note that if the D_s decay contains two or more K_L^0's, we do not find any K_L^0. Due to the low statistics and large systematic uncertainties, we quote the inclusive K_L^0 results only as a check for K_S^0.

The inclusive yields are listed in Table I. For the K_S^0 modes, the corresponding K_L^0 modes are listed as a comparison. The value of the decay $D_s^+ \to K_L^0 X$ is only for D_s^+ decaying into a single K_L^0. So one should not directly compare the values of $D_s^+ \to K_S^0 X$ and $D_s^+ \to K_L^0 X$ in Table I. One can correct the single K_L^0 inclusive yield by adding two times the inclusive yield of $D_s^+ \to K_L^0 K_L^0 X$ (assuming $\mathcal{B}(D_s^+ \to K_L^0 K_L^0 X) = \mathcal{B}(D_s^+ \to K_S^0 K_S^0 X)$). All the K_L^0 modes are consistent with K_S^0 modes. In the last column of Table I, we show PDG [10] averages, when available.

We have considered several sources of systematic uncertainty. The uncertainty associated with the efficiency for finding a track is 0.3%; an additional 0.6% systematic uncertainty for each kaon track is added [5]. The relative systematic uncertainties for π^0 and K_S^0 efficiencies are 4.2% and 1.8%, respectively. Uncertainties in the charged pion and kaon identification efficiencies are 0.3% per pion and 0.3% per kaon [5]. All efficiencies from Monte Carlo have been corrected to include several known small differences between data and Monte Carlo simulation.

The quark-level diagrams contributing to D_s^+ decay are shown in Fig. 4. We classify "quark-level final states" as $s\bar{s}$ (as would come from Fig. 4(a)), $\bar{s}$ (Fig. 4(b)), $s\bar{s}\bar{s}$ (Fig. 4(c)), $\bar{s}\bar{s}$ (Fig. 4(d)), and "no strange quarks" (Fig. 4(e) and Fig. 4(f)). The $s\bar{s}$ final state is

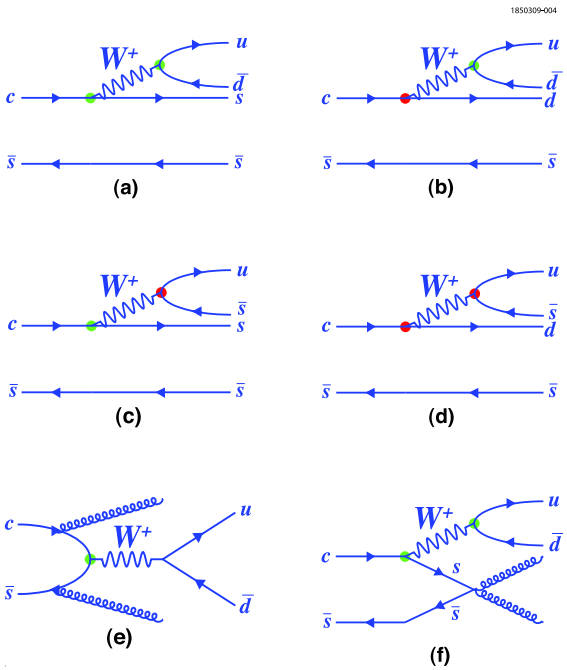

FIG. 4: The typical Feynman diagrams of D_s^+ decays: (a) Cabibbo-favored decay, (b) single-Cabibbo-suppressed decay, (c) single-Cabibbo-suppressed decay, (d) double-Cabibbo-suppressed decay, (e) short-range annihilation decay, (f) long-range annihilation decay.

Cabibbo-favored. The $\bar{s}$ and $s\bar{s}\bar{s}$ final states are singly-Cabibbo-suppressed, the $\bar{s}\bar{s}$ final state is doubly-Cabibbo-suppressed, and the "no strange quarks" final state arises from short-range (Fig. 4(e)) and long-range (Fig. 4(f)) annihilation diagrams (While Fig. 4(f) shows the $s\bar{s}$ annihilating into gluons, here we also include its rescattering into $u\bar{u}$ or $d\bar{d}$).

The $s\bar{s}$ final state can hadronize as $K\bar{K}X$, but also as ηX, $\eta' X$, or ϕX. The $\bar{s}$ final state will hadronize as KX. The $s\bar{s}\bar{s}$ final state in principle can hadronize as $KK\bar{K}X$, but there will be limited phase space for this, so $K\eta X$, $K\eta' X$, $K\phi X$ are probably more likely. The $\bar{s}\bar{s}$ final state will hadronize as KKX, but being doubly-Cabibbo-suppressed, can probably be ignored.

We have performed a global fit to our measurements. For this, we have branching fractions $\mathcal{B}(XX)$. In particular, for $s\bar{s}$ quark-level final states, we write $\mathcal{B}(D_s \to s\bar{s}) \equiv \mathcal{B}(s\bar{s})$, $\mathcal{B}(D_s \to s\bar{s} \to \eta X) \equiv \mathcal{B}(\eta)$, $\mathcal{B}(D_s \to s\bar{s} \to \eta' X) \equiv \mathcal{B}(\eta')$, $\mathcal{B}(D_s \to s\bar{s} \to \phi X) \equiv \mathcal{B}(\phi)$, and $\mathcal{B}(D_s \to s\bar{s} \to K\bar{K}X) \equiv \mathcal{B}(K\bar{K})$. Thus $\mathcal{B}(s\bar{s}) = \mathcal{B}(\eta) + \mathcal{B}(\eta') + \mathcal{B}(\phi) + \mathcal{B}(K\bar{K})$. Note that $\mathcal{B}(D_s \to s\bar{s} \to \eta X)$ is the branching fraction for *primary* production of η (*not* from η' decay), from the quark-level state $s\bar{s}$. The free parameters in our fit are $\mathcal{B}(\eta)$, $\mathcal{B}(\eta')$, $\mathcal{B}(\phi)$, and $\mathcal{B}(K\bar{K})$, which we adjust to obtain the best fit.

For the $\bar{s}$ quark-level final state, we note that $\mathcal{B}(D_s \to \bar{s}) \equiv \mathcal{B}(\bar{s}) \approx |V_{\rm cd}/V_{\rm cs}|^2 \times \mathcal{B}(s\bar{s})$. Thus, we do not adjust $\mathcal{B}(\bar{s})$ in the fit, but write $\mathcal{B}(\bar{s}) = C_1 \times |V_{\rm cd}/V_{\rm cs}|^2 \times \mathcal{B}(s\bar{s})$, where C_1 is a phase space correction factor, probably a bit larger than 1.0. We take C_1 to be 1.25 ± 0.25.

We break the $s\bar{s}\bar{s}$ quark-level final state into 4 separate pieces, as we have done with the $s\bar{s}$ final state. Thus $\mathcal{B}(D_s \to s\bar{s}\bar{s}) \equiv \mathcal{B}(s\bar{s}\bar{s})$ is made up of $\mathcal{B}(D_s \to s\bar{s}\bar{s} \to \eta\bar{s}X) \equiv \mathcal{B}(\eta\bar{s})$, $\mathcal{B}(D_s \to s\bar{s}\bar{s} \to \eta'\bar{s}X) \equiv \mathcal{B}(\eta'\bar{s})$, $\mathcal{B}(D_s \to s\bar{s}\bar{s} \to \phi\bar{s}X) \equiv \mathcal{B}(\phi\bar{s})$, and $\mathcal{B}(D_s \to s\bar{s}\bar{s} \to K\bar{K}\bar{s}X) \equiv \mathcal{B}(K\bar{K}\bar{s})$. Thus $\mathcal{B}(s\bar{s}\bar{s}) = \mathcal{B}(\eta\bar{s}) + \mathcal{B}(\eta'\bar{s}) + \mathcal{B}(\phi\bar{s}) + \mathcal{B}(K\bar{K}\bar{s})$. We note that $\mathcal{B}(s\bar{s}\bar{s}) \approx |V_{\rm us}/V_{\rm ud}|^2 \times \mathcal{B}(s\bar{s})$. So again, we do not adjust any of the pieces making up $\mathcal{B}(s\bar{s}\bar{s})$,

but rather write

$$\mathcal{B}(\eta\bar{s}) = C_2 \times |V_{\rm us}/V_{\rm ud}|^2 \times \mathcal{B}(\eta) \quad (1)$$

$$\mathcal{B}(\eta'\bar{s}) = C_2 \times |V_{\rm us}/V_{\rm ud}|^2 \times \mathcal{B}(\eta') \quad (2)$$

$$\mathcal{B}(\phi\bar{s}) = C_2 \times |V_{\rm us}/V_{\rm ud}|^2 \times \mathcal{B}(\phi) \quad (3)$$

$$\mathcal{B}(K\bar{K}\bar{s}) = C_2 \times |V_{\rm us}/V_{\rm ud}|^2 \times \mathcal{B}(K\bar{K}) \quad (4)$$

The quantity C_2, like C_1, is a phase space correction factor, expected to be smaller than 1.0. We take it to be 0.75 ± 0.25. Assuredly the true phase space correction factors would be different for η, η', ϕ, and $K\bar{K}$. We neglect this in our fit, allowing for it as a systematic error.

For the doubly-Cabibbo-suppressed decays, we estimate $\mathcal{B}(D_s \to \bar{s}\bar{s}) \equiv \mathcal{B}(\bar{s}\bar{s}) = C_3 \times |(V_{\rm cd}/V_{\rm cs})(V_{\rm us}/V_{\rm ud})|^2 \times \mathcal{B}(s\bar{s})$. This term is down a factor of 400 from the dominant term, and has essentially no effect on our fit. We take $C_3 = 1.0 \pm 1.0$.

Finally, there are annihilation diagrams. We write $\mathcal{B}(\text{Annihilation}) = \mathcal{B}(D_s^+ \to \mu^+\nu) + \mathcal{B}(D_s^+ \to \tau^+\nu) + \mathcal{B}(D_s^+ \to \text{Other Annihilation})$. One of our goals in performing the global fit is to get an estimate of $\mathcal{B}(D_s^+ \to \text{Other Annihilation})$. In our fit, we use $\mathcal{B}(D_s^+ \to \tau^+\nu) = (5.62 \pm 0.41 \pm 0.16)\%$ [11], and $\mathcal{B}(D_s^+ \to \mu^+\nu) = (0.565 \pm 0.045 \pm 0.017)\%$ [14].

It is possible for a D_s decay to contain more than one of η, η', ϕ, $K\bar{K}$, *e.g.* $\eta\eta$, $\eta\phi$, etc. From energy conservation, one of an allowed pair must be η. So, we include a yield $\mathcal{B}(\text{extra } \eta)$ to allow for this. We searched for $D_s^+ \to \eta\eta X$, $D_s^+ \to \eta\eta' X$, and $D_s^+ \to \eta\phi X$. We found no clear signals, obtaining a summed yield of $(6.0 \pm 3.9)\%$. In our global fit, we take $\mathcal{B}(\text{extra } \eta)$ to be 6.0%, and include the $\pm 3.9\%$ in the systematic error.

Another source of η and η' is the quark-level decay $D_s \to \bar{s}$ (Fig. 4(b)). Here, the η or η' will come not from their $s\bar{s}$ component, but from their $u\bar{u}$ and $d\bar{d}$ components. At quark level, the decay is $D_s \to u\bar{d}d\bar{s}$, so making η or η' is natural. We assume that this diagram gives an η a fraction f_1 of the time, and an η' a fraction f_2 of the time, where $f_1 + f_2 \leq 1$. While one can make quark-level predictions of what to expect for f_1 and f_2, we take the conservative position of allowing them the full range, $0 \leq f_1 + f_2 \leq 1$, and take $f_1 = f_2 = 1/4$, in the middle of the allowed range.

For our global fit, we write

$$\begin{aligned}
\chi^2 = \; & \Big(\frac{\mathrm{Y}_\eta - (\mathcal{B}(\eta) + \mathcal{B}(\eta\bar{s}) + \mathcal{B}(\eta' \to \eta X) \times (\mathcal{B}(\eta') + \mathcal{B}(\eta'\bar{s}) + f_2 \times \mathcal{B}(\bar{s})) + \mathcal{B}(\text{extra } \eta) + f_1 \times \mathcal{B}(\bar{s}))}{\delta_{\mathrm{Y}_\eta}}\Big)^2 + \\
& \Big(\frac{\mathrm{Y}_{\eta'} - (\mathcal{B}(\eta') + \mathcal{B}(\eta'\bar{s}) + f_2 \times \mathcal{B}(\bar{s}))}{\delta_{\mathrm{Y}_{\eta'}}}\Big)^2 + \\
& \Big(\frac{\mathrm{Y}_\phi - (\mathcal{B}(\phi) + \mathcal{B}(\phi\bar{s}))}{\delta_{\mathrm{Y}_\phi}}\Big)^2 + \\
& \Big(\frac{\mathrm{Y}_{KK} - (\mathcal{B}(K\bar{K}) + \mathcal{B}(K\bar{K}\bar{s}) + \mathcal{B}(\phi \to K\bar{K}) \times (\mathcal{B}(\phi) + \mathcal{B}(\phi\bar{s})) + \mathcal{B}(\bar{s}\bar{s}))}{\delta_{\mathrm{Y}_{KK}}}\Big)^2 + \\
& \Big(\frac{\mathrm{Y}_K - (2 \times (\mathcal{B}(K\bar{K}) + \mathcal{B}(K\bar{K}\bar{s})) + 2 \times \mathcal{B}(\phi \to K\bar{K}) \times (\mathcal{B}(\phi) + \mathcal{B}(\phi\bar{s})) + \mathcal{B}(s\bar{s}\bar{s}) + \mathcal{B}(\bar{s}) + 2 \times \mathcal{B}(\bar{s}\bar{s}))}{\delta_{\mathrm{Y}_K}}\Big)^2
\end{aligned} \quad (5)$$

Here Y_i is the central value of a measurement, and δ_{Y_i} is the error on that measurement. As η' decays to η, and ϕ decays to $K\bar{K}$, our χ^2 needs the branching fractions for those decays, $\mathcal{B}(\eta' \to \eta X)$ and $\mathcal{B}(\phi \to K\bar{K})$. We take these from PDG [10]. Better than words, Eq. (5) gives the meaning of the various $\mathcal{B}(XX)$ parameters. Thus, the measured yield of η, Y_η, has contributions from primary production of η from the $s\bar{s}$ quark state ($\mathcal{B}(\eta)$), primary

TABLE II: Results from the global fit. The central values of parameters are listed in second column. The errors: δ_1 is statistical uncertainty, δ_2 is from phase space factor $C_1 = 1.25 \pm 0.25$, δ_3 is from phase space factor $C_2 = 0.75 \pm 0.25$, δ_4 is from $f_1 + f_2 = 0.5 \pm 0.5$, and δ_5 is from the $\mathcal{B}(\text{extra } \eta) = (6.0 \pm 3.9)\%$.

Parameter	Value(%)	Error(%)				
		δ_1	δ_2	δ_3	δ_4	δ_5
$\mathcal{B}(D_s \to s\bar{s} \to \eta X)$	14.7	2.9	0.2	0.2	1.0	3.7
$\mathcal{B}(D_s \to s\bar{s} \to \eta' X)$	10.3	1.7	0.2	0.1	1.0	0.1
$\mathcal{B}(D_s \to s\bar{s} \to \phi X)$	15.1	1.0	0.0	0.2	0.0	0.0
$\mathcal{B}(D_s \to s\bar{s} \to K\bar{K}X)$	25.4	1.2	0.3	0.6	0.1	0.1
$\mathcal{B}(D_s \to s\bar{s})$	65.6	2.7	0.7	1.0	1.8	3.5
$\mathcal{B}(\text{Other Annihilation})$	21.5	2.8	0.1	0.3	2.0	3.9

production of η from the $s\bar{s}\bar{s}$ quark state ($\mathcal{B}(\eta\bar{s})$), primary production of η from the $\bar{s}$ quark state ($f_1 \times \mathcal{B}(\bar{s})$), production of η from decay of η', the η' being from the $s\bar{s}$ quark state ($\mathcal{B}(\eta') \times \mathcal{B}(\eta' \to \eta X)$), or the η' being from the $s\bar{s}\bar{s}$ quark state ($\mathcal{B}(\eta'\bar{s}) \times \mathcal{B}(\eta' \to \eta X)$), or from the $\bar{s}$ quark state ($f_2 \times \mathcal{B}(\bar{s}) \times \mathcal{B}(\eta' \to \eta X)$), and finally of "extra η's", η that accompanies an η, η', or ϕ already recorded ($\mathcal{B}(\text{extra } \eta)$). The measured yields for η' and ϕ, while not as complicated, have some of the same features. Note that, as described earlier, our measured yield of di-kaons, Y_{KK}, includes $K\bar{K}$ and KK and $\bar{K}\bar{K}$ pairs. There is a subtlety in the last line of Eq. (5). The decay $D_s \to s\bar{s}\bar{s}$ always makes at least one kaon, and when the decay is $D_s \to K\bar{K}\bar{s}$, i.e., $\mathcal{B}(K\bar{K}\bar{s})$, makes 2 more. Line 5, for the kaon yield, properly handles this.

We minimize χ^2 by varying $\mathcal{B}(\eta)$, $\mathcal{B}(\eta')$, $\mathcal{B}(\phi)$, and $\mathcal{B}(K\bar{K})$. All other $\mathcal{B}(XX)$ parameters are fixed as previously described. Further, we have the unitarity requirement $\mathcal{B}(s\bar{s})+\mathcal{B}(s\bar{s}\bar{s})+\mathcal{B}(\bar{s}) + \mathcal{B}(\bar{s}\bar{s}) + \mathcal{B}(\text{Annihilation}) = 1.0$. Our fit gives $\mathcal{B}(\eta)$, $\mathcal{B}(\eta')$, $\mathcal{B}(\phi)$, $\mathcal{B}(K\bar{K})$, and hence $\mathcal{B}(s\bar{s})$, $\mathcal{B}(s\bar{s}\bar{s})$, $\mathcal{B}(\bar{s})$, and $\mathcal{B}(\bar{s}\bar{s})$. Unitarity then gives $\mathcal{B}(\text{Other Annihilation})$. Results are given in Table II.

We have five measurements, and four free parameters. So it would appear that there is one degree of freedom. However, the single kaon and di-kaon measurements are highly correlated, so we effectively have more like four measurements. This is reflected in the χ^2 of the fit, which is 0.03. We have also made a fit leaving the di-kaon term out, and a fit leaving the single kaon term out. These fits give essentially the same result as the nominal fit with both terms included.

In interpreting the results in Table II, it should be recognized that the decay products of the true "other annihilation" diagrams will include some $D_s \to$ gluons $\to s\bar{s}$ events, thus being treated as part of $\mathcal{B}(s\bar{s})$ rather than "other annihilation". Also, the gluons will make $u\bar{u}$, $d\bar{d}$, which will sometimes make η, η', again being treated as a contribution to $\mathcal{B}(s\bar{s})$. Thus $\mathcal{B}(\text{Other Annihilation})$ should be viewed as a lower bound, $\mathcal{B}(\eta)$, $\mathcal{B}(\eta')$, $\mathcal{B}(\phi)$, $\mathcal{B}(K\bar{K})$ as upper bounds, on contributions from the various diagrams in Fig. 4. On the other hand, an overestimate of $\mathcal{B}(\text{extra } \eta)$ will give an overestimate of $\mathcal{B}(\text{Other Annihilation})$.

We can obtain a conservative lower bound on $\mathcal{B}(\text{Other Annihilation})$ by setting $f_1 = f_2 = 0$ and $\mathcal{B}(\text{extra } \eta) = 0$. That gives $\mathcal{B}(\text{Other Annihilation}) = 13.3 \pm 3.0\%$, i.e., $> 9.5\%$ at 90% C.L..

We use our measurements of the total kaon yield and the total di-kaon yield to get a measurement of the singly-Cabibbo-suppressed rate. If there were no tri-kaon events, then (total kaon yield) minus 2×(total di-kaon yield) would give (single kaon yield) which would include the $\bar{s}$ final state, and that fraction of the $s\bar{s}\bar{s}$ final state for which the $s\bar{s}$ component hadronized as η, η', or ϕ. Tri-kaon events complicate the situation. As mentioned earlier, in counting di-kaons, a given charge pairing (K^+K^+, $K^+K^0_S$, K^+K^- etc.) is counted once. Thus $K^0_SK^0_SK^0_SX$ is counted as one di-kaon, while $K^+K^0_SK^0_SX$ is counted as two, $K^+K^0_SK^-X$ as three. For the total kaon yield, a tri-kaon event is counted as 3 kaons, In taking (total kaon yield) minus 2×(total di-kaon yield) as a way of counting singly-Cabibbo-suppressed yield, the "right" answer for a tri-kaon event is +1, and what we actually obtain is +1, −1, and −3, for the different tri-kaon events, on average −1 instead of +1. Thus, our proposed procedure will underestimate the singly-Cabibbo-suppressed rate. To the extent that the tri-kaon rate is small, the underestimate is small. We estimate and apply a correction.

Our numbers are: total kaon yield is $(85.6 \pm 2.3)\%$, total di-kaon yield is $(39.9 \pm 1.8)\%$. The errors are *highly* correlated. Taking correlations into consideration, we find kaon − 2×di-kaon is $(5.8 \pm 2.2)\%$. Taking $\mathcal{B}(s\bar{s}\bar{s})/\mathcal{B}(s\bar{s})$ to be $\sim 1/20$, and $\mathcal{B}(s\bar{s}\bar{s} \to \text{tri-kaon})/\mathcal{B}(s\bar{s}\bar{s})$ to be $< \mathcal{B}(K\bar{K})/\mathcal{B}(s\bar{s}) = 0.39$, our correction factor for the presence of tri-kaon decays is $< (65.6 \times \frac{1}{20} \times 0.39 \times 2)\%$. Thus, the correction factor is $< 2.6\%$. Taking it to be $(1.3 \pm 1.3)\%$, the measured branching fraction for $D_s \to$ single-Cabibbo-suppressed is $(7.1 \pm 2.2 \pm 1.3)\%$. The expected branching fraction is $(|V_{\rm us}/V_{\rm ud}|^2 + |V_{\rm cd}/V_{\rm cs}|^2) \times \mathcal{B}(s\bar{s}) \approx \frac{1}{10} \times \mathcal{B}(s\bar{s})$. Taking $\mathcal{B}(s\bar{s})$ from Table II, we see fine agreement between expectations and measurements.

From our global fit, we can compute the minimum yields of π^+, π^-, and π^0 for each category. For example, for the Cabibbo-favored decay $D^+_s \to s\bar{s} \to \eta X$, with 14.7% yield, we compute the yields of π^+, π^-, and π^0 that come from a 14.7% η yield. To this we add 14.7% π^+ yield, since that must be present to conserve charge. (This is an overestimate, because semileptonic decays have charge conserved via e^+ or μ^+, consequently we perform a subtraction to allow for that.) For $D^+_s \to s\bar{s}\bar{s} \to \eta\bar{s}X$, with 0.6% yield, similarly we compute the yields of π^+, π^-, and π^0 that come from a 0.6% η yield. Charge conservation might be achieved by a π^+, but also by a K^+. Lacking any information on how much comes from π^+, how much from K^+, we assume half from each. Our global fit gives a single number $\mathcal{B}(K\bar{K}) = 25.4\%$, for the di-kaon yield. To determine the π^+, π^0, and π^- yields, we need yields for the separate di-kaon combinations, $K^0_SK^0_S$, $K^0_SK^+$, $K^0_SK^-$, etc. For our calculation, we take the measured di-kaon yields from Table I, and normalize them so their sum equals $\mathcal{B}(K\bar{K})$. (Where we have only an upper limit, we use half of it for the "measurement").

The results of our computation are given in Table III. There one sees that the yields of π^+, π^-, and π^0 should be larger than 96.2%, 20.5%, and 46.8%, respectively. The observed yields are indeed larger than these numbers. Thus, on average, 1/4 of the D_s decays will contain an additional $\pi^+\pi^-$ pair, and 3/4 of the D_s decays will contain an additional π^0 (or 1/2 contain one additional π^0, 1/8 contain two additional π^0's).

For the 21.5% yield of $D_s \to$ Other Annihilation decays, we know nothing about the pion content other than that there will be one π^+ to conserve charge. One might reasonably expect that a substantial fraction of the 1/4 of the D_s decays containing an additional $\pi^+\pi^-$ pair would be in the "Other Annihilation" decays. As for the additional π^0 in 3/4 of the decays, that can appear any place, e.g., as converting a charge-conserving π^+ into a ρ^+. They will probably appear disproportionally in the "Other Annihilation" decays, as these start (in our table) with fewer particles.

The inclusive ω yield, $D_s \to \omega X$, of $6.1 \pm 1.4\%$, is substantial. While ω has an $s\bar{s}$

TABLE III: The minimum yields of π^+, π^-, and π^0 for each category. We compute the yields of π^+, π^-, and π^0 that come from signal particles. In addition to that, we add charged pions to conserve charge. Semileptonic decays have charge conserved via e^+ or μ^+, consequently we perform a subtraction to allow for that.

		Charge Conservation		Particle Decay			Total Yields		
Mode	$\mathcal{B}$ (%)	π^+	π^-	π^+	π^-	π^0	π^+	π^-	π^0
$D_s^+ \to \eta X$	14.7	14.7	0.0	4.0	4.0	17.7	18.7	4.0	17.7
$D_s^+ \to \eta \bar{s} X$	0.6	0.3	0.0	0.2	0.2	0.7	0.4	0.2	0.7
$D_s^+ \to \eta' X$	10.3	10.3	0.0	9.7	9.7	12.7	20.0	9.7	12.7
$D_s^+ \to \eta' \bar{s} X$	0.4	0.2	0.0	0.4	0.4	0.5	0.6	0.4	0.5
$D_s^+ \to \phi X$	15.1	15.1	0.0	2.4	2.4	2.5	17.5	2.4	2.5
$D_s^+ \to \phi \bar{s} X$	0.6	0.3	0.0	0.1	0.1	0.1	0.4	0.1	0.1
$D_s^+ \to$ Extra ηX	6.0	0.0	0.0	1.6	1.6	7.2	1.6	1.6	7.2
$D_s^+ \to \bar{s} X$ (no η, η')	2.1	1.0	0.0	0.0	0.0	0.0	1.0	0.0	0.0
$D_s^+ \to \bar{s} X, X \to \eta$	1.0	0.5	0.0	0.3	0.3	1.2	0.8	0.3	1.2
$D_s^+ \to \bar{s} X, X \to \eta'$	1.0	0.5	0.0	1.0	1.0	1.3	1.5	1.0	1.3
$D_s^+ \to K_S^0 K_S^0 (K_L^0 K_L^0) X$	3.3	3.3	0.0	0.0	0.0	0.0	3.3	0.0	0.0
$D_s^+ \to K_S^0 K^+ (K_L^0 K^+) X$	11.4	0.0	0.0	0.0	0.0	0.0	0.0	0.0	0.0
$D_s^+ \to K_S^0 K^- (K_L^0 K^-) X$	3.7	7.5	0.0	0.0	0.0	0.0	7.5	0.0	0.0
$D_s^+ \to K^+ K^- (-\phi) X$	7.9	7.9	0.0	0.0	0.0	0.0	7.9	0.0	0.0
$D_s^+ \to K^+ K^+ X$	0.1	0.0	0.1	0.0	0.0	0.0	0.0	0.1	0.0
$D_s^+ \to K^- K^- X$	0.03	0.1	0.0	0.0	0.0	0.0	0.1	0.0	0.0
$D_s^+ \to K_S^0 K_L^0 (-\phi) X$	0.0	0.0	0.0	0.0	0.0	0.0	0.0	0.0	0.0
$D_s^+ \to e^+ (\mu^+) X$	10.7	-10.7	0.0	0.0	0.0	0.0	-10.7	0.0	0.0
$D_s^+ \to \tau^+ \nu$	5.6	0.0	0.0	4.1	0.8	2.9	4.1	0.8	2.9
$D_s^+ \to \mu^+ \nu$	0.6	0.0	0.0	0.0	0.0	0.0	0.0	0.0	0.0
$D_s^+ \to$ Other Annihilation	21.5	21.5	0.0	0.0	0.0	0.0	21.5	0.0	0.0
Minimum Yields							96.2	20.5	46.8
Observed Yields							119.3	43.2	123.4
Additional Yields							23.0	22.7	76.7

component, it is *very* small, so it is unlikely that very much of the ω yield comes from the $s\bar{s}$ component of $D_s^+ \to s\bar{s}X$. At quark level, this is $D_s^+ \to s\bar{s}u\bar{d}$, and a decay $D_s^+ \to \pi^+\eta\omega$ is quite possible. A decay $D_s^+ \to \pi^+\eta'\omega$, from energy considerations, is just barely possible. From the decay $D_s^+ \to s\bar{s}\bar{s}$, ω could come from $D_s^+ \to K^+\eta\omega$ (barely), but not from $D_s^+ \to K^+\eta'\omega$. From $D_s^+ \to \bar{s}X$, it can come from $D_s^+ \to K^+\omega X$, with lots of phase space. And from "Other Annihilation", there are lots of possibilities. In summary, with the data we now have in hand, we can not say much about the origin of the 6% ω yield. A search for D_s^+ *exclusive* decays will be reported in a separate paper. (We should note that our inclusive ω measurement came towards the end of the work described here, and so was *not* included in the retuning of the Monte Carlo decay table. CLEO's D_s Monte Carlo decay table produces far fewer ω's than the 6% we observe.)

In summary, we report several measurements of D_s^+ inclusive decays with significantly

better precision than current world averages.

We gratefully acknowledge the effort of the CESR staff in providing us with excellent luminosity and running conditions. D. Cronin-Hennessy and A. Ryd thank the A.P. Sloan Foundation. This work was supported by the National Science Foundation, the U.S. Department of Energy, the Natural Sciences and Engineering Research Council of Canada, and the U.K. Science and Technology Facilities Council.

---

[1] R. A. Briere *et al.* (CESR-c and CLEO-c Taskforces, CLEO-c Collaboration), Cornell University, LEPP Report No. CLNS 01/1742 (2001) (unpublished).
[2] Y. Kubota *et al.* (CLEO Collaboration), Nucl. Instrum. Meth. A **320**, 66 (1992).
[3] D. Peterson *et al.*, Nucl. Instrum. Methods Phys. Res., Sec. A **478**, 142 (2002).
[4] M. Artuso *et al.*, Nucl. Instrum. Methods Phys. Res., Sec. A **502**, 91 (2003).
[5] S. Dobbs *et al.* (CLEO Collaboration), Phys. Rev. D **76**, 112001 (2007).
[6] R. Brun *et al.*, GEANT 3.21, CERN Program Library Long Writeup W5013 (unpublished) 1993.
[7] D.J. Lange, Nucl. Instrum. Methods Phys. Res., Sec. A **462**, 152 (2001).
[8] E. Barberio and Z. Wąs, Comput. Phys. Commun. **79**, 291 (1994).
[9] D. Cronin-Hennessy *et al.* (CLEO Collaboration), arXiv:0801.3418.
[10] W.-M. Yao *et al.* (Particle Data Group), J. Phys. G **33**, 1 (2006).
[11] P. U. E. Onyisi *et al.* (CLEO Collaboration), Phys. Rev. D **79**, 052002 (2009).
[12] T. E. Coan *et al.* (CLEO Collaboration), Phys. Rev. Lett. **95**, 181802 (2005).
[13] T. Skwarnicki, Ph.D thesis, Institute for Nuclear Physics, Krakow, Poland, 1986.
[14] J. P. Alexander *et al.* (CLEO Collaboration), Phys. Rev. D **79**, 052001 (2009).